Biochemical Pharmacology 85 (2013) 1370–1378

Contents lists available at SciVerse ScienceDirect

Biochemical Pharmacology

journal homepage: www.elsevier.com/locate/biochempharm

Carbonyl reduction of triadimefon by human and rodent 11β-hydroxysteroid dehydrogenase 1

Arne Meyer [a], Anna Vuorinen [b], Agnieszka E. Zielinska [c], Thierry Da Cunha [a], Petra Strajhar [a], Gareth G. Lavery [c], Daniela Schuster [b], Alex Odermatt [a,*]

[a] Swiss Center for Applied Human Toxicology and Division of Molecular and Systems Toxicology, Department of Pharmaceutical Sciences, University of Basel, Klingelbergstrasse 50, 4056 Basel, Switzerland
[b] Institute of Pharmacy/Pharmaceutical Chemistry and Center for Molecular Biosciences Innsbruck – CMBI, University of Innsbruck, Innrain 80/82, 6020 Innsbruck, Austria
[c] Centre for Endocrinology Diabetes and Metabolism (CEDAM), Institute of Biomedical Research, Medical School Building, School of Clinical and Experimental Medicine, College of Medical and Dental Sciences, University of Birmingham, Edgbaston, Birmingham B15 2TT, UK

ARTICLE INFO

Article history:
Received 22 December 2012
Accepted 8 February 2013
Available online 16 February 2013

Keywords:
Triadimefon
11β-Hydroxysteroid dehydrogenase
Metabolism
Liver microsomes
Azole fungicide
Molecular docking

ABSTRACT

11β-Hydroxysteroid dehydrogenase 1 (11β-HSD1) catalyzes the conversion of inactive 11-oxo glucocorticoids (endogenous cortisone, 11-dehydrocorticosterone and synthetic prednisone) to their potent 11β-hydroxyl forms (cortisol, corticosterone and prednisolone). Besides, 11β-HSD1 accepts several other substrates. Using rodent liver microsomes and the unspecific inhibitor glycyrrhetinic acid, it has been proposed earlier that 11β-HSD1 catalyzes the reversible conversion of the fungicide triadimefon to triadimenol. In the present study, recombinant human, rat and mouse enzymes together with a highly selective 11β-HSD1 inhibitor were applied to assess the role of 11β-HSD1 in the reduction of triadimefon and to uncover species-specific differences. To further demonstrate the role of 11β-HSD1 in the carbonyl reduction of triadimefon, microsomes from liver-specific 11β-HSD1-deficient mice were employed. Molecular docking was applied to investigate substrate binding. The results revealed important species differences and demonstrated the irreversible 11β-HSD1-dependent reduction of triadimefon. Human liver microsomes showed 4 and 8 times higher activity than rat and mouse liver microsomes. The apparent V_{max}/K_m of recombinant human 11β-HSD1 was 5 and 15 times higher than that of mouse and rat 11β-HSD1, respectively, indicating isoform-specific differences and different expression levels for the three species. Experiments using inhibitors and microsomes from 11β-HSD1-deficient mice indicated that 11β-HSD1 is the major if not only enzyme responsible for triadimenol formation. The IC_{50} values of triadimefon and triadimenol for cortisone reduction suggested that exposure to these xenobiotica unlikely impairs the 11β-HSD1-dependent glucocorticoid activation. However, elevated glucocorticoids during stress or upon pharmacological administration likely inhibit 11β-HSD1-dependent metabolism of triadimefon in humans.

1. Introduction

Triadimefon and to a lesser extent the active metabolite triadimenol are used as broad-spectrum fungicides in agriculture and landscaping, with annual application rates of about 135,000 and 24,000 lbs/year, respectively [1]. Humans can be exposed through consumption of foods containing triadimefon or triadimenol residues [2]. More critical is occupational exposure through dermal contact and inhalation of sprays by field workers applying these fungicides [3]. The wide use of triadimefon and its long half-life of around 23 days under controlled laboratory conditions [4] emphasizes the need to investigate both the environmental fate and the potentially hazardous effects on animals and humans.

Toxicological studies revealed neurotoxic effects of triadimefon and triadimenol in rats, mice and rabbits [1]. Teratogenic effects were observed at very low concentrations in experiments using rat embryos [5]. Furthermore, triadimefon and triadimenol were shown to cause thyroid and liver tumors in rats, and they are considered as potential human carcinogens [1]. They act by inhibiting the activity of fungal lanosterol-14α-demethylase, a cytochrome P450 enzyme (CYP51), thereby blocking ergosterol biosynthesis which is essential for fungal cell wall integrity [6]. Like other azole fungicides, triadimefon and triadimenol can inhibit some of the mammalian cytochrome P450 enzymes involved in steroidogenesis, which may lead to endocrine disturbances [7].

* Corresponding author. Tel.: +41 61 267 1530; fax: +41 61 267 1515.
E-mail address: alex.odermatt@unibas.ch (A. Odermatt).

0006-2952/$ – see front matter © 2013 Elsevier Inc. All rights reserved.
http://dx.doi.org/10.1016/j.bcp.2013.02.014

According to conclusions by the US Environmental Protection Agency (EPA), the mechanisms of toxicity of triadimefon and triadimenol differ from those of other azole fungicides [1]. Kenneke et al. proposed that differences in the metabolism of triadimefon compared with other azole fungicides may be involved [8]. Experiments by Barton et al. with liver microsomes revealed that triadimefon can be metabolized by CYPs, whereby CYP2B6, CYP2C19 and CYP3A4 were the most active enzymes in human liver [9]. The authors mentioned very low formation of triadimenol; however, they used assay conditions that do not allow to measure luminal carbonyl reductase activity. Kenneke et al., using rat liver microsomes and the unselective inhibitor glycyrrhetinic acid, then provided evidence that triadimefon is mainly metabolized to triadimenol and that this reaction is catalyzed by 11β-hydroxysteroid dehydrogenase 1 (11β-HSD1, SDR26C1) [8,10,11]. Interestingly, in a follow-on study they reported the conversion of triadimefon to triadimenol by rainbow trout microsomes [12], although it is known that the gene encoding 11β-HSD1 is absent in teleost species [13], thus suggesting the involvement of another enzyme.

11β-HSD1 plays a pivotal role in the regulation of energy metabolism through the activation of endogenous glucocorticoids in tissues such as liver, adipose and skeletal muscle [14]. Moreover, it essentially regulates the balance of mineralocorticoid receptor (MR)- and glucocorticoid receptor (GR)-mediated modulation of inflammatory parameters in macrophage-derived cells [15–17]. 11β-HSD1 is required for the pharmacological effect of cortisone and prednisone, which do not bind to corticosteroid receptors. Since 11β-HSD1 is considered as a promising target for the treatment of metabolic disorders, there is great interest in the development of 11β-HSD1 inhibitors [14,18]. Besides its role in glucocorticoid activation, 11β-HSD1 catalyzes the carbonyl reduction of several endogenous oxidized sterols such as 7-ketocholesterol [19,20], 7-ketodehydroepiandrosterone [21] and the secondary bile acid 7-oxolithocholic acid [22], as well as that of several xenobiotics including oracin [23], metyrapone [24], ketoprofen [25], 4-(methylnitrosamino)-1-(3-pyridyl)-1-butanone (NNK) [26], and as mentioned above, triadimefon [8,10,11].

Since the evidence for a role of 11β-HSD1 in the metabolism of triadimefon was based on rat microsomal activities and inhibition by the unselective inhibitor glycyrrhetinic acid (GA), we aimed in the present study to (1) optimize the assay conditions to distinguish between luminal enzymes and microsomal enzymes facing the cytoplasm, (2) compare carbonyl reduction activity in human, rat and mouse liver microsomes in the presence and absence of a selective 11β-HSD1 inhibitor, (3) assess whether other enzymes contribute to the carbonyl reduction of triadimefon in human, rat and mouse liver microsomes, (4) assess activities of the corresponding recombinant 11β-HSD1 enzymes, and (5) investigate the binding of triadimefon to 11β-HSD1 by molecular modeling.

2. Materials and methods

2.1. Chemicals and reagents

Human liver microsomes were purchased from Celsis In Vitro Inc. (Baltimore, MD) and were obtained from a 77 year old male Caucasian. Human embryonic kidney (HEK-293) cells from ATCC (No. CRL-1573) were obtained through LGC Standards S.a.r.l., Molsheim Cedex, France. Cell culture medium was from Invitrogen (Carlsbad, CA) and 5H-1,2,4-triazolo(4,3-a)azepine,6,7,8,9-tetrahydro-3-tricyclo(3·3·1·13·7)dec-1-yl (T0504) from Enamine (Kiev, Ukraine). BNW16 was kindly provided by Dr. Thomas Wilckens, BioNetWorks GmbH, Munich, Germany. Steroids were purchased from Steraloids (Newport, RI). Triadimefon, triadimenol, glycyrrhetinic acid (GA) and all other chemicals were from Sigma–Aldrich Chemie GmbH (Buchs, Switzerland). The solvents were of analytical and high performance liquid chromatography grade and the reagents of the highest grade available.

2.2. Cell culture, transfection and enzyme expression

HEK-293 cells were cultivated in Dulbecco's modified Eagle medium (DMEM) containing 4.5 g/L glucose, 10% fetal bovine serum, 100 U/mL penicillin, 0.1 mg/mL streptomycin, 1× MEM non-essential amino acids and 10 mM HEPES buffer, pH 7.4. Cells were incubated at 37 °C in a humidified 5% CO_2 atmosphere. Cells were transiently transfected by the calcium phosphate transfection method with plasmids for C-terminally FLAG-tagged human, rat or mouse 11β-HSD1 [27], or human 11β-HSD2 [28]. Briefly, HEK-293 cells at 70% confluence on a 10 cm^2 dish with 10 mL of culture medium were transfected with 10 μg plasmid. The plasmid was diluted in 430 μL sterile water, followed by drop wise addition of 62.5 μL of 2 M $CaCl_2$. This mixture was then added drop wise to 500 μL BEST buffer (500 mL H_2O containing 8.0 g NaCl, 0.198 g Na_2HPO_4-heptahydrate, 5.3 g BES (N,N-bis[2-hydroxyethyl]-2-amino ethane sulfonic acid), pH 7.0). After incubation for 10 min at room temperature, this mixture was added to the cells. Medium was changed at 6 h post-transfection. The transfection efficiency was approximately 20%. Cells were trypsinized 48 h post-transfection, followed by centrifugation at 900 × *g* for 4 min. Cell pellets (4 pellets per 10 cm^2 dish) were immediately shock frozen on dry ice and stored at −80 °C. Upon determination of the protein concentration using the Pierce BCA protein assay kit (Thermo Fisher Scientific Inc., Rockford, IL, USA), 20 μg of total protein were loaded onto SDS-PAGE and expression of FLAG-tagged enzymes was semi-quantitatively analyzed by Western blotting and immune-detection using mouse monoclonal M2 anti-FLAG antibody (Sigma–Aldrich Chemie GmbH) and horseradish peroxidase-conjugated secondary antibodies as described previously [29]. β-Actin was used as a loading control and was detected using rabbit anti-actin IgG from Santa Cruz Biotechnology Inc. (Santa Cruz, CA, USA).

2.3. Preparation of liver microsomes

Sprague-Dawley rats were obtained from Charles River, Paris, France, and housed in the breeding facility of the Biocenter, University of Basel, in groups of four in a 12:12-h light–dark cycle with standard laboratory chow and tap water ad libitum. Mice on a mixed C57BL/6J/129vJ background and liver-specific knock-out mice (LKO) generated by crossing albumin-Cre transgenic mice on a C57BL/6J background with floxed homozygous *HSD11B1* mice on a mixed C57BL/6J/129SvJ background were bred at the breeding facility of the University of Birmingham, UK, as described earlier [30]. Pooled microsomes were prepared from the livers of three adult male Sprague-Dawley rats or three C57BL/6J/129vJ parental mice or LKO mice. Liver pieces were homogenized in solution A (0.3 M sucrose, 10 mM imidazole, pH 7.0; 2 mL per 100 mg tissue) with a Potter-Elvehjem PTFE pestle with 10–12 strokes and at 220 rpm. Debris and nuclei were removed by two centrifugation steps for 10 min at 1000 × *g*. The supernatant was centrifuged twice for 10 min at 12,000 × *g* to remove mitochondria, followed by ultracentrifugation for 1 h at 100,000 × *g* to obtain microsomes. The pellet was resuspended in solution B (0.6 M potassium chloride, 0.3 M sucrose, 20 mM Tris–maleate, pH 7.0; 500 μL per 100 mg tissue) and the ultracentrifugation step was repeated. The final pellet was resuspended in solution C (0.15 M potassium chloride, 0.25 M sucrose, 10 mM Tris–maleate, pH 7.0; 200 μL per 100 mg tissue). The microsomes were then aliquoted, shock frozen on dry ice and stored at −80 °C until further use. The microsomal

protein concentration was measured using the Pierce BCA protein assay kit. The quality of the microsomal preparations was analyzed using the cytochrome C reductase assay kit (Sigma–Aldrich Chemie GmbH) and by assessing the latent activity of the 11β-HSD1-dependent oxoreduction of cortisone in the presence of glucose-6-phosphate (G6P).

2.4. Determination of enzyme activities using microsomal preparations

In order to measure the oxoreduction of cortisone, microsomes of human liver (final concentration (f.c.) 0.5 mg/mL), rat liver (f.c. 0.25 mg/mL), mouse liver (f.c. 0.5 mg/mL) and LKO mouse liver (f.c. 0.5 mg/mL) were incubated in a final reaction volume of 22 μL of TS2 buffer (100 mM NaCl, 1 mM EGTA, 1 mM EDTA, 1 mM $MgCl_2$, 250 mM sucrose, 20 mM Tris–HCl, pH 7.4), supplemented with 1 μM cortisone and either 1 mM G6P or 1 mM NADPH in the presence or absence of 20 μM of the selective 11β-HSD1 inhibitor T0504 for 15 min at 37 °C. For measuring the metabolism of triadimefon, 1 μM triadimefon and rat liver microsomes (f.c. 1 mg/mL), mouse liver microsomes (f.c. 1 mg/mL) or human liver microsomes (f.c. 0.2 mg/mL) were incubated for 1 h at 37 °C. Reactions were stopped by the addition of 200 μL 0.3 M zinc sulfate in a 1:1 (v/v) mixture of water and methanol. The internal standard (atrazine for triadimefon and deuterized d4-cortisol for cortisone) was added at a final concentration of 50 nM, followed by vortexing for 10 s and centrifugation for 10 min at 12,000 × *g* on a table top centrifuge. Supernatants (180 μL) were transferred onto solid phase extraction columns (Oasis HBL 1 cc (30 mg) Waters WAT094225, Waters, Milford, MA, USA) pre-conditioned with 1 mL of methanol and 1 mL of distilled water. After washing with 1 mL water, compounds were eluted with 1 mL methanol. The eluate was evaporated to dryness, reconstituted in 100 μL methanol and stored at −20 °C until analysis by liquid chromatography–tandem mass spectrometry (LC–MS/MS) (Section 2.6).

2.5. Determination of enzyme activities using lysates of transfected HEK-293 cells

Frozen pellets of HEK-293 cells transiently transfected with human, rat or mouse 11β-HSD1 were resuspended in TS2 buffer and immediately sonicated at 4 °C using a Branson sonicator (5 pulses, output 2, and duty cycles 20). Lysates were incubated for 1 h at 37 °C in the presence of 1 mM NADPH and different concentrations of triadimefon (8 μM, 4 μM, 2 μM, 1 μM, 500 nM, 250 nM and 125 nM) in a final volume of 22 μL to estimate apparent K_m and apparent V_{max} values for the three species. Substrate conversion in all experiments was kept below 25%. Reactions were stopped and processed as described in Section 2.4.

Alternatively, the oxidation of triadimenol was assessed by incubating lysates of cells, transiently transfected with human 11β-HSD1 or 11β-HSD2 (SDR9C3), with 1 μM triadimenol and 1 mM $NADP^+$ to measure the oxidation capacity of 11β-HSD1, or with 1 μM triadimenol and 1 mM NAD^+ to measure 11β-HSD2 activity. The conversion of cortisol (at a concentration of 1 μM) was determined as a positive control.

For determination of the reductase activity of human 11β-HSD1, cell lysates were incubated in the presence of 1 μM cortisone or 1 μM triadimefon as substrate and various concentrations of either triadimefon and triadimenol or cortisone as the respective inhibitor. IC_{50} values were calculated by non-linear regression using four parametric logistic curve fitting (GraphPad Prism software).

2.6. Liquid chromatography–tandem mass spectrometry measurements

All chromatographic separations (HPLC) were performed using an Atlantis T3 column (3 μm, 2.1 mm × 150 mm, Waters) and an Agilent 1200 Infinity Series chromatograph (Agilent Technologies, Basel, Switzerland). The mobile phase consisted of solvent A (water:acetonitrile, 95:5 (v/v), containing 0.1% formic acid) and solvent B (water:acetonitrile, 5:95 (v/v), containing 0.1% formic acid), at a total flow rate of 0.4 mL/min. Triadimefon and triadimenol were separated using 25% solvent B for 1 min, followed by a linear gradient from 1 to 20 min to reach 70% solvent B, and then 100% solvent B for 3 min. The column was then re-equilibrated with 25% solvent B. Cortisone and cortisol were resolved using 30% solvent B from 0 to 4 min, followed by a linear gradient from 30% solvent B to 40% solvent B from 4 to 7 min, solvent B was then increased to 100% from 7 to 7.5 min and then continued for another 2.5 min, followed by re-equilibration with 30% solvent B for 3 min.

The LC was interfaced to an Agilent 6490 triple quadropole tandem mass spectrometer (MS/MS).

The entire LC–MS/MS system was controlled by Mass Hunter workstation software (version B.01.05). The injection volume of each sample was 10 μL. The mass spectrometer was operated in electrospray ionization (ESI) positive ionization mode, with the source temperature of 350 °C, with nebulizer pressure of 20 psi. The capillary voltage was set at 4000 V.

The compounds were analyzed using multiple-reaction monitoring (MRM) and identified by comparing their retention time and mass to charge ratio (*m*/*z*) with those of authentic standards. The transitions, collision energy and retention time were *m*/*z* 294.8/197, 12 V, 13 min for triadimefon; *m*/*z* 296.8/70, 12 V, 11.0 and 11.5 min (R/S enantiomer) for triadimenol; *m*/*z* 216/174, 16 V, 5 min for atrazine; *m*/*z* 361/163, 25 V, 4.6 min for cortisone; *m*/*z* 363/121, 26 V, 4.3 min for cortisol; and *m*/*z* 367.2/121.1, 36 V, 4.3 min for the internal standard d4-cortisol.

The LC–MS/MS method was validated for accuracy, precision, sensitivity, stability, recovery, and calibration range. Acceptable inter-day assay precision (≤5.2%) and accuracy (95.0–103.9%) were achieved over a linear range of 50–5000 nM for both triadimefon and triadimenol. Recovery of triadimefon was close to 100% and that of triadimenol >60% in all solid phase extractions. For each experiment a new calibration curve was determined.

2.7. Molecular modeling

Triadimefon and triadimenol were docked to the X-ray crystal structure of 11β-HSD1 using AutoDock4 [31]. The 3D-structures of the ligands were downloaded from PubChem [32] (CID-codes: 39385 for triadimefon and 41368 for triadimenol, respectively), and the structure of the protein was obtained from Protein Data Bank (PDB, www.pdb.org [33], entry: 2BEL [34]). The selected protein structure contains the tetrameric form of the protein; however, the docking studies were performed only with chain A. The protein was prepared for docking by removing the cocrystallized ligand carbenoxolone and water molecules from the protein structure as well as by adding hydrogens. The atom types of the protein and the ligands were automatically created by the program. During the docking, the ligand conformations were set flexible (with five rotatable bonds for triadimefon and six for triadimenol, respectively) and the protein was handled as rigid. The binding site was defined as a 3D-grid, centered at the binding site point *X* = 8.858, *Y* = 22.143, and *Z* = 15.547, with 30, 40, and 30 points in the respective dimensions. The grid spacing was set to 0.375 Å. The genetic algorithm was selected as search method with default settings, except for the maximum number of evaluations,

which was set to short (250,000). The default settings for docking run were kept, with one exception: the RMS cluster tolerance was set to 1.0 Å. Using these settings, the docking program was able to reproduce the binding orientation of the cocrystallized ligand, carbenoxolone, which validated the docking settings.

3. Results

3.1. Optimization of assay conditions and measurement of cortisone reduction in liver microsomes

In a first step, the assay conditions were optimized in order to distinguish between NADPH-dependent activities of microsomal enzymes facing the cytoplasm and enzymes facing the ER-lumen. The preparation employed in the present study yielded microsomes with approximately 90% inside-out orientation, based on the latency of 11β-HSD1-dependent reduction of cortisone as well as the latent activity of hexose-6-phosphate dehydrogenase (H6PDH) [35]. Thus, the luminal compartment is protected by the microsomal membrane, and enzymes with a cytoplasmic orientation such as CYPs and 17β-HSD1 or 17β-HSD3 can be readily measured upon addition of NADPH to the reaction mixture [36]. A NADPH regenerating system using bacterial G6PDH and G6P, widely used for measurements of CYP activities, further stimulates microsomal enzymes with cytoplasmic orientation when high substrate concentrations (>10 μM) are applied. In contrast, carbonyl reductases such as 11β-HSD1 that protrude into the ER-lumen are dependent on the NADPH pool present in the microsomal vesicle [37–39]. The high endogenous expression of H6PDH in the liver represents an endogenous NADPH regenerating system, and we found that the addition of G6P to the assay mixture was required and sufficient to stimulate 11β-HSD1 reductase activity. Due to the relatively small vesicle volume, the capacity of this endogenous regenerating system is limited, however, and substrate concentrations have to be kept below 5–10 μM. Therefore, a substrate concentration of 1 μM was chosen for the experiments with liver microsomes.

A comparison of the cortisone reduction in human, rat and mouse liver microsomes yielded comparable activities of human and mouse liver microsomes and approximately 2-fold higher activity of rat microsomes ($p < 0.001$) (Fig. 1). The latency of 11β-HSD1 activity was about 90% for rat and mouse microsomes and about 75% for the commercially available human liver microsomes (data not shown). To compare the activity of liver microsomes from wild-type and 11β-HSD1-deficient mice, cytochrome C reductase activity was determined. Comparable activities were obtained for microsomes of wild-type and knock-out mice with 3.35 U/mL and 3.13 U/mL, respectively. Importantly, microsomes of 11β-HSD1-deficient mice were devoid of cortisone reductase activity as expected, and cortisone reductase activity in hepatic microsomes from wild-type mice was completely blocked upon coincubation with the selective 11β-HSD1 inhibitor T0504.

3.2. Reduction of triadimefon in liver microsomes

In the presence of G6P triadimefon was efficiently converted to triadimenol by mouse liver microsomes (Fig. 2). In contrast, much lower activity was detected when microsomes were incubated with NADPH ($p < 0.001$), an activity corresponding to the low percentage of right-side out vesicles. Importantly, the conversion of triadimefon to triadimenol could be completely blocked with the specific 11β-HSD1 inhibitors T0504 (Fig. 2) and BNW16 (not shown) as well as with the unspecific inhibitor glycyrrhetinic acid (GA). Further excluding the possibility that other enzymes might be involved in the observed carbonyl reduction of triadimefon,

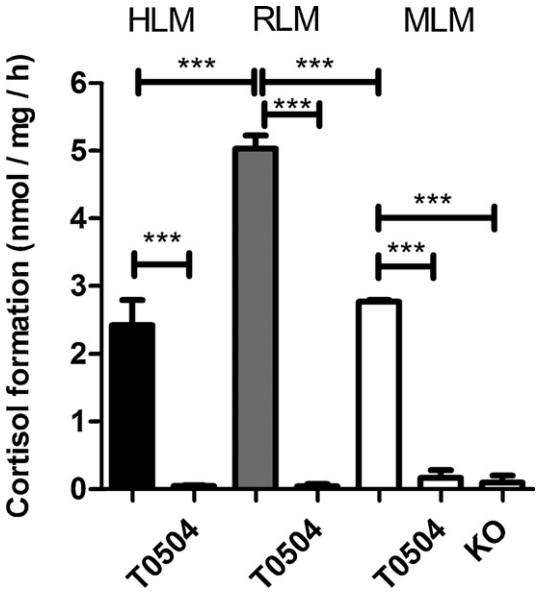

Fig. 1. Conversion of cortisone to cortisol by liver microsomes. Human liver microsomes (HLM, black bars, f.c. 0.5 mg/mL), rat liver microsomes (RLM, gray bars, f.c. 0.25 mg/mL) and mouse liver microsomes (MLM, white bars, f.c. 0.5 mg/mL) were incubated for 15 min at 37 °C in the presence of 1 μM cortisone and 1 mM glucose-6-phosphate, in the absence or presence of 20 μM of the 11β-HSD1 inhibitor T0504. The amount of cortisone and cortisol was then quantitated. Lack of activity of liver microsomes from 11β-HSD1-deficient mice is indicated by KO. Data (mean ± SD) were obtained from at least three independent experiments using pooled samples. Repeated measures ANOVA found significant species differences in cortisone reduction. Post hoc analysis by Tukey test was used for multiple comparisons. $^{***}p < 0.001$.

microsomes of liver-specific 11β-HSD1 knock-out mice showed no conversion of triadimefon to triadimenol.

A species comparison revealed about 4-fold higher triadimefon carbonyl reductase activity of human liver microsomes compared with rat liver microsomes ($p < 0.001$) and 8-fold higher activity

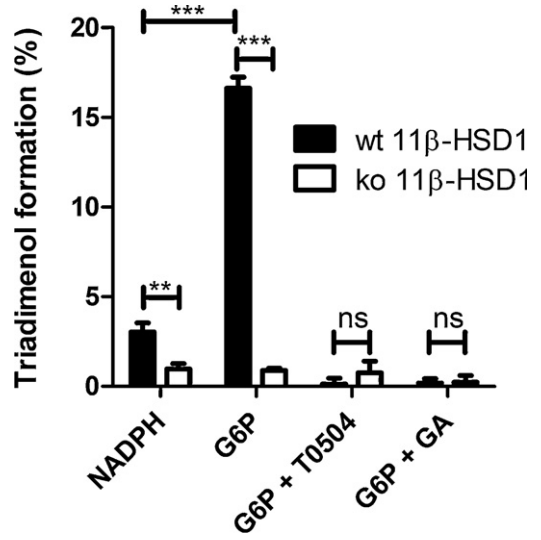

Fig. 2. Conversion of triadimefon to triadimenol by mouse liver microsomes. Microsomes (1 mg/mL), prepared from wild-type (wt) and liver-specific 11β-HSD1 knock-out mice (ko), were incubated for 1 h at 37 °C in the presence of 1 μM triadimefon and either 1 mM of NADPH or 1 mM of glucose-6-phosphate (G6P), in the absence or presence of 20 μM T0504 or glycyrrhetinic acid (GA). Data represent mean ± SD from at least three independent experiments using pooled samples. Repeated measures ANOVA found significant differences in the groups. Post hoc analysis by Tukey test was used for multiple comparisons. $^{**}p < 0.01$, $^{***}p < 0.001$, ns = not significant.

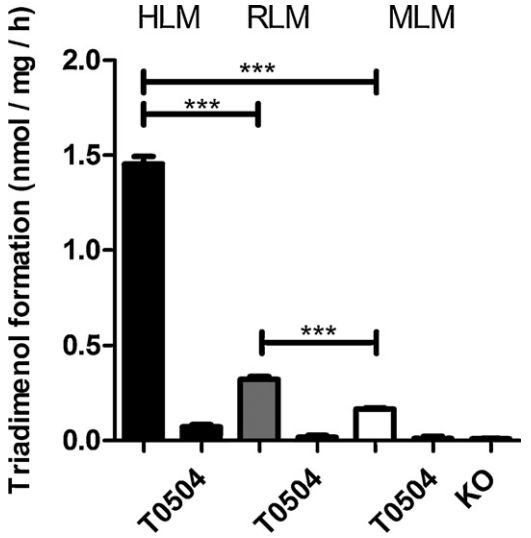

Fig. 3. Triadimenol formation in liver microsomes. Human liver microsomes (HLM, black bars, f.c. 0.2 mg/mL), rat liver microsomes (RLM, gray bars, f.c. 1 mg/mL) and mouse liver microsomes (MLM, white bars, f.c. 1 mg/mL) were incubated for 1 h at 37 °C with 1 μM triadimefon and 1 mM G6P, in the absence or presence of 20 μM T0504. Lack of activity of MLM of 11β-HSD1-deficient mice is indicated by KO. Data (mean ± SD) were obtained from at least three independent experiments using pooled samples. Repeated measures ANOVA found significant species differences in triadimefon reduction. Post hoc analysis by Tukey test was used for multiple comparisons. $^{***}p < 0.001$.

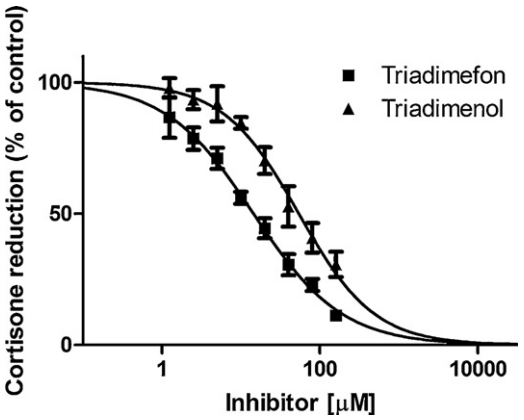

Fig. 4. Inhibition of 11β-HSD1-dependent triadimefon reduction by cortisone. Inhibition of the 11β-HSD1-dependent conversion of triadimefon to triadimenol by various concentrations of cortisone was measured in lysates of HEK-293 cells transfected with the human enzyme as described in Section 2. Lysates were simultaneously incubated with triadimefon (1 μM) and cortisone for 60 min at 37 °C. Data were normalized to vehicle control (0.05% DMSO) and represent mean ± SD from three independent experiments.

than mouse liver microsomes ($p < 0.001$) (Fig. 3). The fact that the selective inhibitor T0504 completely abolished triadimefon reductase activity indicated that 11β-HSD1 is the major if not only microsomal enzyme catalyzing this reaction.

3.3. Reduction of triadimefon by recombinant 11β-HSD1 measured in cell lysates

The different microsomal activities can potentially be due to differences in 11β-HSD1 expression levels, differences in the expression of H6PDH and/or its interaction with 11β-HSD1, or species-specific differences in the kinetic properties of 11β-HSD1. Significant species-specific differences in the substrate and inhibitor specificity of 11β-HSD1 have been reported [27,40]. Therefore, in a next step, the carbonyl reduction of triadimefon by recombinant human, rat and mouse 11β-HSD1 was measured in lysates of transiently transfected HEK-293 cells. HEK-293 cells were chosen because they do not express endogenous steroid-metabolizing enzymes and to be able to compare the enzymes of the three species in the same cellular background. Because HEK-293 cells express no or very low H6PDH levels [37], lysates were prepared by sonication, which leads to microsomal vesicles with mixed orientation and allows measuring 11β-HSD1 activity in the presence of NADPH. Lysates of untransfected HEK-293 cells did not metabolize triadimefon. A comparison of the triadimefon reduction revealed a 3–4-fold higher affinity of human compared with rat and mouse 11β-HSD1 (Table 1). The expression levels of 11β-HSD1 in transiently transfected cells were semi-quantitatively analyzed by Western blotting and densitometry and did not vary significantly between species (data not shown). Human 11β-HSD1 was most active with 2-fold and 4-fold higher V_{max} and 5-fold and 15-fold higher V_{max}/K_m values than mouse and rat 11β-HSD1, respectively (Table 1).

3.4. Inhibition of 11β-HSD1-dependent cortisone reduction by triadimefon and vice versa

In order to estimate the potential of triadimefon and triadimenol to interfere with glucocorticoid activation, inhibition of human 11β-HSD1-dependent cortisone reduction by the azole fungicides was measured. IC_{50} values of 15.3 ± 7.0 μM and 56 ± 14 μM were obtained for triadimefon and triadimenol, respectively (Fig. 4). The 11β-HSD1-dependent reduction of triadimefon was inhibited by cortisone with an IC_{50} of 289 ± 54 nM (Fig. 5).

3.5. 11β-HSD1 and 11β-HSD2 do not catalyze the oxidation of triadimenol

11β-HSD1 is a reversible enzyme in vitro and catalyzes the interconversion of cortisone/cortisol, 11-dehydrocorticosterone/corticosterone, prednisone/prednisolone, 7β-hydroxycholesterol/7-oxocholesterol, and 7α- and 7β-hydroxydehydroepiandrosterone/7-oxodehydroepiandrosterone [41]. However, we reported recently that 11β-HSD1 irreversibly catalyzes the reduction of the secondary bile acid 7-oxolithocholic acid to chenodeoxycholic acid [22]. Therefore, the potential oxidation of triadimenol by

Table 1
Kinetic parameters of 11β-HSD1-dependent carbonyl reduction of triadimefon. HEK-293 cells were transiently transfected with either human, rat or mouse 11β-HSD1, followed by measuring the carbonyl reduction of triadimefon and determination of apparent V_{max} and apparent K_m values as described in Section 2. The appV_{max} values are expressed relative to total protein concentration of the lysates used. Data were calculated by non-linear regression using four parametric logistic curve fitting (GraphPad Prism) and represent mean ± SD of three independent experiments. One-way ANOVA found significant differences ($p < 0.01$) in appV_{max} values, post hoc analysis by Tukey test was used for multiple comparisons. Human appV_{max} value was significant higher than rat appV_{max} ($p < 0.01$) and mouse appV_{max} ($p < 0.05$). Other comparisons were not significant.

11β-HSD1	appV_{max}	appK_m	appV_{max}/appK_m
Human	0.54 ± 0.060 nmol × mg^{-1} × h^{-1}	3.5 ± 0.8 μM	154 × 10^{-6} l × mg^{-1} × h^{-1}
Rat	0.14 ± 0.031 nmol × mg^{-1} × h^{-1}	12.8 ± 4.2 μM	11 × 10^{-6} l × mg^{-1} × h^{-1}
Mouse	0.31 ± 0.129 nmol × mg^{-1} × h^{-1}	10.4 ± 6.5 μM	30 × 10^{-6} l × mg^{-1} × h^{-1}

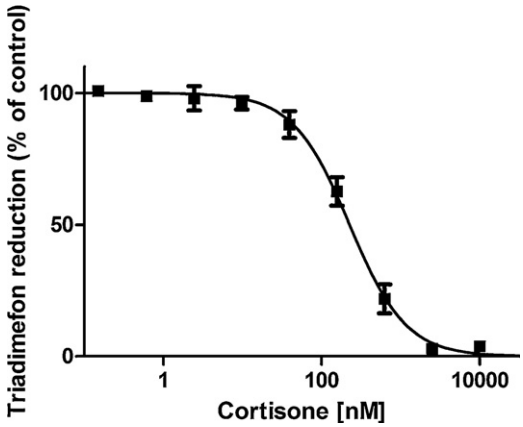

Fig. 5. Inhibition of 11β-HSD1-dependent cortisone reduction by triadimefon and triadimenol. Inhibition of the 11β-HSD1-dependent conversion of cortisone to cortisol by various concentrations of triadimefon and triadimenol was measured in lysates of HEK-293 cells transfected with the human enzyme as described in Section 2. Lysates were simultaneously incubated with cortisone (1 μM) and triadimefon or triadimenol for 15 min at 37 °C. Data were normalized to vehicle control (0.05% DMSO) and represent mean ± SD from three independent experiments.

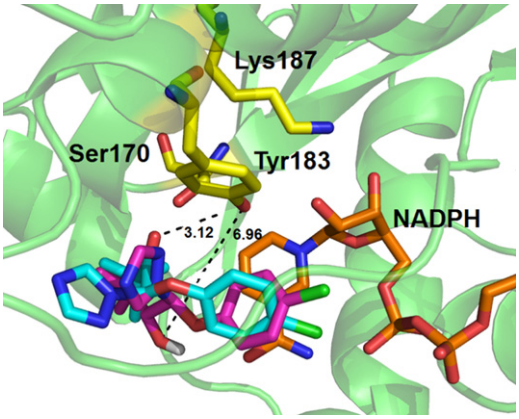

Fig. 7. The binding orientations of triadimefon (cyan) and triadimenol (magenta) in the 11β-HSD1 binding site. The carbonyl-oxygen of triadimefon is facing toward catalytic residues, with a distance of the hydroxyl on Tyr183 to the carbonyl-oxygen of 3.12 Å. Triadimenol is predicted to have a flipped binding orientation, where the reduced carbonyl-oxygen faces away from the catalytic residues, with a distance of the hydroxyl on Tyr183 to the carbonyl-oxygen of 6.96 Å.

11β-HSD1 was tested in the presence of the cofactor $NADP^+$. Triadimenol was not oxidized by 11β-HSD1 (Fig. 6). As a control to verify enzyme activity, the reduction of triadimefon was measured, resulting in efficient formation of triadimenol, with 70% substrate conversion. Furthermore, incubation of triadimenol with lysates of cells expressing 11β-HSD2 in the presence of NAD^+ did not result in the formation of any triadimefon. Under similar conditions, cortisol was converted by 90% to cortisone (not shown).

3.6. Analysis of the binding of triadimefon and triadimenol to 11β-HSD1 by molecular modeling

Using molecular docking, the binding orientations were predicted for triadimefon and triadimenol. The binding orientation of triadimefon is comparable to that reported by Mazur et al. [10], while triadimenol is observed in the binding pocket in a flipped way compared with triadimefon (Fig. 7). Triadimefon is located in the binding pocket with the carbonyl-oxygen facing toward the catalytic amino acids Tyr183 and Ser170, and forming hydrogen bonds with them (Fig. 8A and B). In contrast, triadimenol is located in the same area with the alcohol group pointing away from Tyr183 and Ser170 (Fig. 8A, C and D). Instead, the alcohol group forms a hydrogen bond with the cofactor molecule.

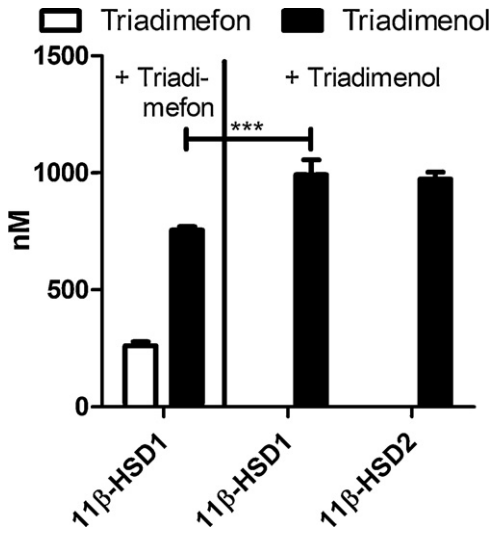

Fig. 6. Triadimenol is not oxidized by 11β-HSD1 and 11β-HSD2. Recombinant human 11β-HSD1 and 11β-HSD2 were expressed in HEK-293 cells. Cells were lysed by sonication to obtain vesicles with mixed orientation. 11β-HSD1 activity was measured by incubation of lysates for 1 h at 37 °C with 1 μM triadimefon and 1 mM NADPH or with 1 μM triadimenol and 1 mM $NADP^+$. 11β-HSD2 activity was measured in the presence of 1 μM triadimenol and 1 mM NAD^+. Data (mean ± SD) were obtained from at least three independent experiments. Repeated measures ANOVA found significant differences. Post hoc analysis by Tukey test was used for multiple comparisons. $^{***}p < 0.001$.

4. Discussion

Almost all studies on the assessment of NADPH-dependent enzyme activities reported in the literature so far used either NADPH or an NADPH-regenerating system (NRS), consisting of $NADP^+$, G6P and purified bacterial G6PDH. Mazur et al. compared different conditions to measure 11β-HSD1 reductase activity and observed highest activity upon incubation of microsomes with an NRS in the presence of the pore forming agent alamethicin [10]. However, in this setting NADPH is produced in the extra-vesicular space and can be readily utilized by cytochrome P450 enzymes.

In the present study, optimized assay conditions have been applied to distinguish between activities of NADPH-dependent microsomal enzymes facing the cytoplasm and enzymes protruding into the ER luminal compartment. Intact liver microsomes contain an endogenous NRS, consisting of the luminal pyrimidine nucleotide pool, the glucose-6-phosphate translocase (G6PT) and H6PDH. Because of the neglectible permeability of the ER membrane for pyridine nucleotides, the NADPH generated by H6PDH upon addition of G6P into the assay buffer is exclusively available for ER luminal enzymes. The intactness of microsomal vesicles and the percentage of inside-out vesicles (approximately 90% in the protocol used) can be tested by comparing 11β-HSD1-dependent cortisone reduction in the presence of either NADPH or G6P. The quality of microsomal preparations can be further assessed by measuring cytochrome C reductase activity. This approach should be valuable for the characterization of enzymatic conditions of other luminal carbonyl reductases.

In mouse liver microsomes the NADPH-dependent conversion of triadimefon to metabolites other than triadimenol was almost two times higher than the G6P-dependent formation of triadimenol. This ratio was significantly different in rat and human liver microsomes, where the carbonyl reduction of triadimefon was

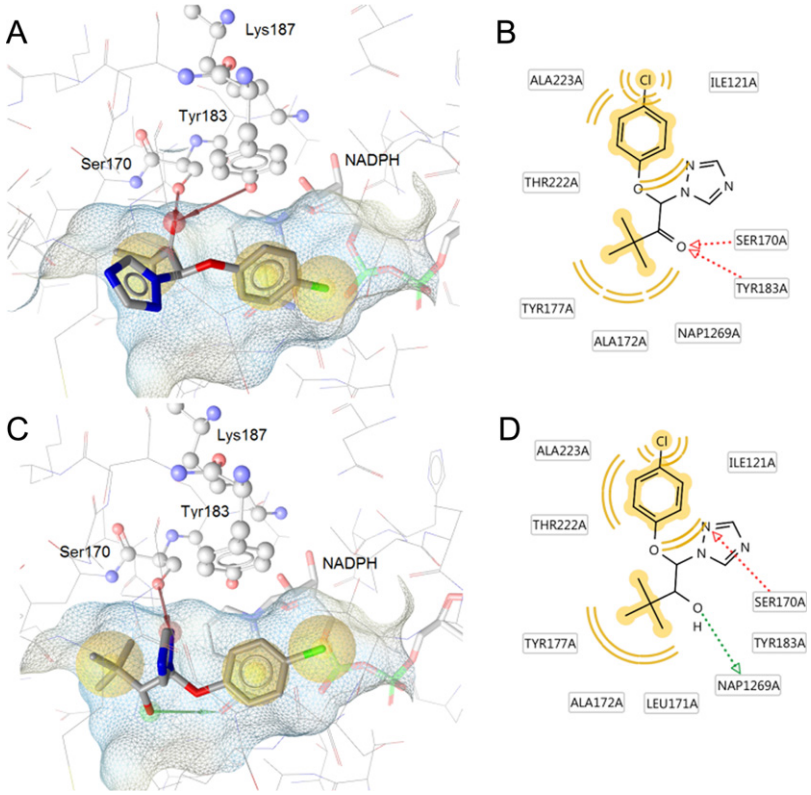

Fig. 8. The predicted binding orientations of triadimefon (A and B) and triadimenol (C and D) in 11β-HSD1. The ligand–protein interactions are color-coded: hydrogen bond acceptor – red arrow, hydrophobic – yellow sphere. The ligand binding pocket is colored by aggregated lipophilicity. The catalytic amino acids are highlighted in ball- and stick style and the cofactor NADPH in stick style.

2- and 8-fold higher than in mice. The cytochrome P450-mediated metabolism of triadimefon has been described earlier [9,42]. Barton et al. reported a role for cytochrome P450 subfamilies 2C and 3A in the hydroxylation of triadimefon by rat liver microsomes [9]. Iyer et al. identified the two metabolites 1-(4-chlorophenoxy)-4-hydroxy-3,3-dimethyl-1-(1H-1,2,4-triazol-1-yl)-2-butanone (kwg1323) and β-(4-chlorophenoxy)-α-(1,1-dimethylethyl)-1H-1,2,4-triazole-1-ethanol (desmethyl kwg1342) in experiments using cultured rat hepatocytes.

The use of selective 11β-HSD1 inhibitors demonstrates that the carbonyl reduction of triadimefon is catalyzed exclusively by 11β-HSD1. This is further substantiated by the fact that no triadimenol formation could be observed in microsomes from livers of 11β-HSD1-deficient mice. The analysis of the kinetic properties of recombinant 11β-HSD1 revealed clearly higher triadimefon reductase activity of the human isoform compared with the rodent isoforms. Although it must be taken into consideration that the rat and mouse enzymes were expressed in a human cell line, and that it cannot be fully excluded that the lower activities might emerge from protein folding disturbances, or the lack of some mouse- or rat-specific factors in human cells, comparable cortisone reductase activities for the three enzymes have been observed in this cell system in previous experiments [27]. The present study revealed similar affinities for triadimefon of rat and mouse 11β-HSD1. The fact that the recombinant mouse enzyme had 3-fold higher catalytic efficiency (V_{max}/K_m) than the rat enzyme but rat microsomes were twice as active as mouse microsomes (in line with a previous study by Crowell et al. [11]) suggests a higher expression of 11β-HSD1 in rats. Indeed, approximately two times higher cortisone reductase activity was obtained in rat liver microsomes compared with mouse liver microsomes. A reliable comparison of 11β-HSD1 protein expression levels in human, rat and mouse is difficult due to significant species specificity of available antibodies. The present study suggests that rats and mice are of limited use to study the possible consequences of impaired carbonyl reduction of triadimefon for humans; however, 11β-HSD1-deficient mice turned out to be very useful for solving mechanistic questions.

Crowell et al. recently developed a physiologically based pharmacokinetic model for triadimefon and triadimenol in rats and humans [43]. The model showed good results for peak blood and tissue levels, but the clearance of both compounds was over estimated. Better results were obtained by a reverse metabolism model, based on the assumption that 11β-HSD1, or alternatively 11β-HSD2, might catalyze the oxidation of triadimenol. However, our results revealed that neither 11β-HSD1 nor 11β-HSD2 catalyze the oxidation of triadimenol. Previous studies demonstrated that 11β-HSD1 is a reversible enzyme that catalyzes the interconversion of endogenous glucocorticoids as well as 7-oxigenated cholesterol and 7-oxigenated DHEA in vitro, and molecular modeling revealed the close proximity of the carbonyl and the respective hydroxyl on C7 and C11 of the steroid backbone to the catalytic Tyr183 [21,44,45]. However, a recent study reported the irreversible reduction of 7-oxolithocholic acid by 11β-HSD1, whereby molecular modeling suggested that only 7-oxolithocholic acid has optimal binding of substrate and cofactor to Tyr183 and Lys187, thus allowing electron transfer with the cofactor [22]. Similarly, the docking studies of the present study support our experimental findings that triadimenol is not oxidized by 11β-HSD1 (Figs. 7 and 8). Triadimefon binds to 11β-HSD1 in an orientation, where the carbonyl-oxygen is pointing toward the catalytic amino acids Tyr183 and Ser170, and forming hydrogen bonds with them. This orientation is essential, since in the reduction reaction, the hydrogen is transferred from Tyr183 to the substrate [46]. Thus, the binding orientation of triadimefon allows the reduction reaction to take place. In contrast, triadimenol has a

flipped binding mode compared to triadimefon, suggesting why this compound is not oxidized by 11β-HSD1. These findings suggest that after reduction of triadimefon to triadimenol, the compound rotates away from the catalytic amino acids, thus preventing its oxidation. However, the fact that triadimenol fits to the binding pocket and forms hydrogen bonds with the catalytic amino acid Ser170 and the cofactor, could explain the weak inhibitory activity of this compound.

In an attempt to estimate whether exposure to triadimefon or triadimenol might affect 11β-HSD1-dependent glucocorticoid activation, we determined IC_{50} values of the two fungicides for cortisone reduction. Regarding the expected exposure levels upon intake of contaminated food or water or upon occupational exposure of field workers and uptake through skin, it is highly unlikely that concentrations as high as 10 μM are reached to significantly inhibit 11β-HSD1-dependent cortisone reduction. On the other side, cortisone efficiently inhibited the carbonyl reduction of triadimefon. Under the conditions applied, an apparent K_m of 300–400 nM for cortisone reduction has been obtained [47]. Thus, the IC_{50} of about 300 nM obtained in the present study suggests that at elevated concentrations of 11-oxoglucocorticoids, i.e. during stress situations or therapeutic treatment, the carbonyl reduction of triadimefon may be significantly lowered. The competition of cortisone (or 11-dehydrocorticosterone) and triadimefon for binding to 11β-HSD1 may explain the lower than expected clearance of triadimefon based on the physiologically based pharmacokinetic model in the study by Crowell et al. [43]. The observation suggests that the circadian rhythm of glucocorticoids should be considered for estimation of the clearance of triadimefon.

In conclusion, the use of recombinant enzymes demonstrated the ability of 11β-HSD1 to irreversibly catalyze the carbonyl reduction of triadimefon. Comparison of human, rat and mouse 11β-HSD1 revealed at least five times higher catalytic efficiency of the human compared with the rodent enzymes, which is relevant regarding an improved cross-species extrapolation for risk assessment. Absence of triadimenol formation upon incubation of microsomes from livers of 11β-HSD1-deficient mice and of liver microsomal preparations with selective 11β-HSD1 inhibitors indicate that 11β-HSD1 is the major if not only enzyme catalyzing the conversion of triadimefon to triadimenol. Finally, inhibition studies suggest that the carbonyl reduction of triadimefon is impaired by elevated cortisone levels.

Conflict of interest statement

The authors declare that there are no conflicts of interest.

Acknowledgements

This work was supported by the Swiss National Science Foundation (PDFMP3_127330) to Alex Odermatt and a BBSRC David Philips fellowship (BB/G023468/1) to Gareth G. Lavery. Alex Odermatt has a Chair for Molecular and Systems Toxicology by the Novartis Research Foundation. Anna Vuorinen thanks the University of Innsbruck, Nachwuchsförderung for financial support.

References

[1] Agency USEP. Triadimefon reregistration eligibility decision (RED) and triadimenol tolerance reassessment and risk management decision (TRED) fact sheet. In: Office of Pesticide Programs USEPA, editor. Washington, DC; 2006.
[2] Yess NJ, Houston MG, Gunderson EL. Food Drug Administration pesticide residue monitoring of foods: 1983–1986. J Assoc Off Anal Chem 1991;74:273–80.
[3] Lavy TL, Mattice JD, Massey JH, Skulman BW. Measurements of year-long exposure to tree nursery workers using multiple pesticides. Arch Environ Contam Toxicol 1993;24:123–44.
[4] Fang H, Tang FF, Zhou W, Cao ZY, Wang DD, Liu KL, et al. Persistence of repeated triadimefon application and its impact on soil microbial functional diversity. J Environ Sci Health B 2012;47:104–10.
[5] Menegola E, Broccia ML, Di Renzo F, Prati M, Giavini E. In vitro teratogenic potential of two antifungal triazoles: triadimefon and triadimenol. In Vitro Cell Dev Biol Anim 2000;36:88–95.
[6] Robinson JF, Tonk ECM, Verhoef A, Piersma AH. Triazole induced concentration-related gene signatures in rat whole embryo culture. Reprod Toxicol 2012;34:275–83.
[7] Vinggaard AM, Hnida C, Breinholt V, Larsen JC. Screening of selected pesticides for inhibition of CYP19 aromatase activity in vitro. Toxicol In Vitro 2000;14:227–34.
[8] Kenneke JF, Mazur CS, Ritger SE, Sack TJ. Mechanistic investigation of the noncytochrome P450-mediated metabolism of triadimefon to triadimenol in hepatic microsomes. Chem Res Toxicol 2008;21:1997–2004.
[9] Barton HA, Tang J, Sey YM, Stanko JP, Murrell RN, Rockett JC, et al. Metabolism of myclobutanil and triadimefon by human and rat cytochrome P450 enzymes and liver microsomes. Xenobiotica 2006;36:793–806.
[10] Mazur CS, Kenneke JF, Goldsmith M-R, Brown C. Contrasting influence of NADPH and a NADPH-regenerating system on the metabolism of carbonyl-containing compounds in hepatic microsomes. Drug Metab Dispos 2009;37:1801–5.
[11] Crowell SR, Henderson WM, Fisher JW, Kenneke JF. Gender and species differences in triadimefon metabolism by rodent hepatic microsomes. Toxicol Lett 2010;193:101–7.
[12] Kenneke JF, Ekman DR, Mazur CS, Konwick BJ, Fisk AT, Avants JK, et al. Integration of metabolomics and in vitro metabolism assays for investigating the stereoselective transformation of triadimefon in rainbow trout. Chirality 2010;22:183–92.
[13] Baker ME. Evolutionary analysis of 11[beta]-hydroxysteroid dehydrogenase-type 1, -type 2, -type 3 and 17[beta]-hydroxysteroid dehydrogenase-type 2 in fish. FEBS Lett 2004;574:167–70.
[14] Atanasov AG, Odermatt A. Readjusting the glucocorticoid balance: an opportunity for modulators of 11beta-hydroxysteroid dehydrogenase type 1 activity? Endocr Metab Immune Disord Drug Targets 2007;7:125–40.
[15] Chantong B, Kratschmar DV, Nashev LG, Balazs Z, Odermatt A. Mineralocorticoid and glucocorticoid receptors differentially regulate NF-kappaB activity and pro-inflammatory cytokine production in murine BV-2 microglial cells. J Neuroinflammation 2012;9:260.
[16] Chapman KE, Odermatt A. Steroids modulators of inflammation and immunity. J Steroid Biochem Mol Biol 2010;120:67–8.
[17] Staab CA, Maser E. 11beta-Hydroxysteroid dehydrogenase type 1 is an important regulator at the interface of obesity and inflammation. J Steroid Biochem Mol Biol 2010;119:56–72.
[18] Hughes KA, Webster SP, Walker BR. 11-Beta-hydroxysteroid dehydrogenase type 1 (11beta-HSD1) inhibitors in type 2 diabetes mellitus and obesity. Expert Opin Invest drugs 2008;17:481–96.
[19] Schweizer RA, Zurcher M, Balazs Z, Dick B, Odermatt A. Rapid hepatic metabolism of 7-ketocholesterol by 11beta-hydroxysteroid dehydrogenase type 1: species-specific differences between the rat, human, and hamster enzyme. J Biol Chem 2004;279:18415–24.
[20] Hult M, Elleby B, Shafqat N, Svensson S, Rane A, Jornvall H, et al. Human and rodent type 1 11beta-hydroxysteroid dehydrogenases are 7beta-hydroxycholesterol dehydrogenases involved in oxysterol metabolism. Cell Mol Life Sci 2004;61:992–9.
[21] Nashev LG, Chandsawangbhuwana C, Balazs Z, Atanasov AG, Dick B, Frey FJ, et al. Hexose-6-phosphate dehydrogenase modulates 11beta-hydroxysteroid dehydrogenase type 1-dependent metabolism of 7-keto- and 7beta-hydroxyneurosteroids. PLoS ONE 2007;2:e561.
[22] Odermatt A, Da Cunha T, Penno CA, Chandsawangbhuwana C, Reichert C, Wolf A, et al. Hepatic reduction of the secondary bile acid 7-oxolithocholic acid is mediated by 11β-hydroxysteroid dehydrogenase 1. Biochem J 2011;436:621–9.
[23] Wsol V, Szotakova B, Skalova L, Maser E. Stereochemical aspects of carbonyl reduction of the original anticancer drug oracin by mouse liver microsomes and purified 11beta-hydroxysteroid dehydrogenase type 1. Chem Biol Interact 2003;143/144:459–68.
[24] Maser E, Bannenberg G. 11 beta-hydroxysteroid dehydrogenase mediates reductive metabolism of xenobiotic carbonyl compounds. Biochem Pharmacol 1994;47:1805–12.
[25] Hult M, Nobel CS, Abrahmsen L, Nicoll-Griffith DA, Jornvall H, Oppermann UC. Novel enzymological profiles of human 11beta-hydroxysteroid dehydrogenase type 1. Chem Biol Interact 2001;130–132:805–14.
[26] Maser E, Friebertshauser J, Volker B. Purification, characterization and NNK carbonyl reductase activities of 11beta-hydroxysteroid dehydrogenase type 1 from human liver: enzyme cooperativity and significance in the detoxification of a tobacco-derived carcinogen. Chem Biol Interact 2003;143/144:435–48.
[27] Arampatzis S, Kadereit B, Schuster D, Balazs Z, Schweizer RA, Frey FJ, et al. Comparative enzymology of 11beta-hydroxysteroid dehydrogenase type 1 from six species. J Mol Endocrinol 2005;35:89–101.
[28] Odermatt A, Arnold P, Stauffer A, Frey BM, Frey FJ. The N-terminal anchor sequences of 11beta-hydroxysteroid dehydrogenases determine their orientation in the endoplasmic reticulum membrane. J Biol Chem 1999;274:28762–70.
[29] Meyer A, Strajhar P, Murer C, Da Cunha T, Odermatt A. Species-specific differences in the inhibition of human and zebrafish 11beta-hydroxysteroid dehydrogenase 2 by thiram and organotins. Toxicology 2012;301:72–8.

[30] Lavery GG, Zielinska AE, Gathercole LL, Hughes B, Semjonous N, Guest P, et al. Lack of significant metabolic abnormalities in mice with liver-specific disruption of 11beta-hydroxysteroid dehydrogenase type 1. Endocrinology 2012;153:3236–48.
[31] Morris GM, Huey R, Lindstrom W, Sanner MF, Belew RK, Goodsell DS, et al. AutoDock4 and AutoDockTools4: automated docking with selective receptor flexibility. J Comput Chem 2009;30:2785–91.
[32] Bolton E, Wang Y, Thiessen PA, Bryant SH. PubChem: integrated platform of small molecules and biological activities. In: Annual Reports in Computational Chemistry. Washington, DC: American Chemical Society; 2008.
[33] Berman HM, Westbrook J, Feng Z, Gilliland G, Bhat TN, Weissig H, et al. The Protein Data Bank. Nucleic Acids Res 2000;28:235–42.
[34] Wu X, Kavanagh K, Svensson S, Elleby B, Hult M, Von Delft F, et al. The high resolution structures of human, murine and guinea pig 11-beta-hydroxysteroid dehydrogenase type 1 reveal critical differences in active site architecture. DOI:102210/pdb2bel/pdb.
[35] Senesi S, Legeza B, Balazs Z, Csala M, Marcolongo P, Kereszturi E, et al. Contribution of fructose-6-phosphate to glucocorticoid activation in the endoplasmic reticulum: possible implication in the metabolic syndrome. Endocrinology 2010;151:4830–9.
[36] Legeza B, Balazs Z, Nashev LG, Odermatt A. The microsomal enzyme 17beta-hydroxysteroid dehydrogenase 3 faces the cytoplasm and uses NADPH generated by glucose-6-phosphate dehydrogenase. Endocrinology 2013;154:205–13.
[37] Atanasov AG, Nashev LG, Gelman L, Legeza B, Sack R, Portmann R, et al. Direct protein–protein interaction of 11beta-hydroxysteroid dehydrogenase type 1 and hexose-6-phosphate dehydrogenase in the endoplasmic reticulum lumen. Biochim Biophys Acta 2008;1783:1536–43.
[38] Atanasov AG, Nashev LG, Schweizer RA, Frick C, Odermatt A. Hexose-6-phosphate dehydrogenase determines the reaction direction of 11beta-hydroxysteroid dehydrogenase type 1 as an oxoreductase. FEBS Lett 2004;571:129–33.
[39] Banhegyi G, Benedetti A, Fulceri R, Senesi S. Cooperativity between 11beta-hydroxysteroid dehydrogenase type 1 and hexose-6-phosphate dehydrogenase in the lumen of the endoplasmic reticulum. J Biol Chem 2004;279:27017–21.
[40] Hult M, Shafqat N, Elleby B, Mitschke D, Svensson S, Forsgren M, et al. Active site variability of type 1 11beta-hydroxysteroid dehydrogenase revealed by selective inhibitors and cross-species comparisons. Mol Cell Endocrinol 2006;248:26–33.
[41] Odermatt A, Nashev LG. The glucocorticoid-activating enzyme 11β-hydroxysteroid dehydrogenase type 1 has broad substrate specificity: physiological and toxicological considerations. J Steroid Biochem Mol Biol 2010;119:1–13.
[42] Iyer VV, Ovacik MA, Androulakis IP, Roth CM, Ierapetritou MG. Transcriptional and metabolic flux profiling of triadimefon effects on cultured hepatocytes. Toxicol Appl Pharmacol 2010;248:165–77.
[43] Crowell SR, Henderson WM, Kenneke JF, Fisher JW. Development and application of a physiologically based pharmacokinetic model for triadimefon and its metabolite triadimenol in rats and humans. Toxicol Lett 2011;205:154–62.
[44] Balazs Z, Nashev LG, Chandsawangbhuwana C, Baker ME, Odermatt A. Hexose-6-phosphate dehydrogenase modulates the effect of inhibitors and alternative substrates of 11beta-hydroxysteroid dehydrogenase 1. Mol Cell Endocrinol 2009;301:117–22.
[45] Odermatt A, Atanasov AG, Balazs Z, Schweizer RA, Nashev LG, Schuster D, et al. Why is 11beta-hydroxysteroid dehydrogenase type 1 facing the endoplasmic reticulum lumen? Physiological relevance of the membrane topology of 11beta-HSD1. Mol Cell Endocrinol 2006;248:15–23.
[46] Kavanagh KL, Jornvall H, Persson B, Oppermann U. Medium- and short-chain dehydrogenase/reductase gene and protein families: the SDR superfamily: functional and structural diversity within a family of metabolic and regulatory enzymes. Cell Mol Life Sci 2008;65:3895–906.
[47] Frick C, Atanasov AG, Arnold P, Ozols J, Odermatt A. Appropriate function of 11beta-hydroxysteroid dehydrogenase type 1 in the endoplasmic reticulum lumen is dependent on its N-terminal region sharing similar topological determinants with 50-kDa esterase. J Biol Chem 2004;279:31131–38.